Supplement of Atmos. Chem. Phys., 22, 12387–12399, 2022
https://doi.org/10.5194/acp-22-12387-2022-supplement
© Author(s) 2022. CC BY 4.0 License.

Atmospheric Chemistry and Physics
Open Access
EGU

Supplement of

Impact of water uptake and mixing state on submicron particle deposition in the human respiratory tract (HRT) based on explicit hygroscopicity measurements at HRT-like conditions

Ruiqi Man et al.

Correspondence to: Zhijun Wu (zhijunwu@pku.edu.cn)

The copyright of individual parts of the supplement might differ from the article licence.

[Supporting Information]

The particle hygroscopicity parameter (Kappa, κ) in this study and previous studies measured in rural sites in the North China Plain (NCP) is shown in Table S1. The average size-resolved κ was in the range of 0.24−0.32 during the sampling period. The hygroscopic properties of particles in this study was similar to those determined in the NCP in summer, such as in Wuqing (Liu et al., 2011) and Xianghe (Zhang et al., 2016), which was higher than that measured in winter, such as in Dingxing (Shi et al., 2022). It can be explained that the mass fraction of organic matters with relatively weak hygroscopicity was higher in winter, while secondary inorganic aerosols with strong hygroscopicity made higher contribution in summer (Sun et al., 2015). Besides, particle hygroscopicity increased as the particle diameter increasing, which was in accordance with previous studies measured in urban and rural sites (Swietlicki et al., 2008).

Table S 1. Particle hygroscopicity parameter (Kappa, κ) in this study and previous studies.

Rural site	Kappa, mean ± SD (dry diameter, nm)						Instrument	RH	Reference
Wangdu	0.24 ± 0.09 (30)	0.24 ± 0.07 (50)	0.27 ± 0.06 (100)	0.28 ± 0.07 (150)	0.30 ± 0.08 (200)	0.32 ± 0.10 (250)	HH-TDMA	98%	This study
Wuqing	0.25 ± 0.06 (50)	0.28 ± 0.04 (100)	0.33 ± 0.05 (200)	0.35 ± 0.05 (250)			HH-TDMA	98.5%	(Liu et al., 2011)
Xianghe	0.29 ± 0.09 (50)	0.30 ± 0.06 (100)	0.31 ± 0.06 (150)	0.33 ± 0.04 (200)	0.35 ± 0.08 (250)	0.37 ± 0.09 (350)	H-TDMA	87%	(Zhang et al., 2016)
Dingxing	0.16 (60)	0.18 (100)	0.16 (150)	0.15 (200)			H-TDMA	90%	(Shi et al., 2022)

Table S 2. Wet diameters of hydrophobic and hygroscopic particles in the HRT.

Dry diameter (nm)	Wet diameter (mean ± SD, nm)			
	Head		TB/P	
	Hydrophobic	Hygroscopic	Hydrophobic	Hygroscopic
12.6	12.7 ± 0.0	13.4 ± 0.4	13.1 ± 0.2	17.0 ± 2.1
14.2	14.3 ± 0.0	15.2 ± 0.5	14.9 ± 0.3	19.8 ± 2.6
16.1	16.2 ± 0.1	17.2 ± 0.5	17.0 ± 0.3	23.3 ± 3.2
18.2	18.3 ± 0.1	19.5 ± 0.6	19.3 ± 0.4	27.4 ± 3.7
20.5	20.7 ± 0.1	22.1 ± 0.6	22.0 ± 0.5	32.4 ± 4.3
23.2	23.4 ± 0.1	25.1 ± 0.6	25.1 ± 0.6	38.5 ± 4.7
26.2	26.5 ± 0.1	28.5 ± 0.6	28.7 ± 0.8	45.9 ± 5.0
29.7	30.0 ± 0.1	32.4 ± 0.7	32.8 ± 1.0	54.9 ± 5.4
33.6	33.9 ± 0.1	36.7 ± 0.7	37.5 ± 1.3	65.5 ± 5.9
38.0	38.4 ± 0.1	41.7 ± 0.8	42.9 ± 1.6	77.9 ± 6.8
42.9	43.4 ± 0.1	47.2 ± 0.8	49.1 ± 1.9	92.4 ± 7.9
48.5	49.0 ± 0.2	53.5 ± 1.0	56.2 ± 2.4	109.4 ± 9.3
54.9	55.4 ± 0.2	60.6 ± 1.1	64.3 ± 2.9	129.1 ± 11.0
62.0	62.7 ± 0.2	68.7 ± 1.2	73.5 ± 3.5	152.0 ± 12.8
70.2	70.9 ± 0.2	77.8 ± 1.4	83.8 ± 4.0	178.8 ± 14.8
79.3	80.1 ± 0.2	88.1 ± 1.6	95.2 ± 4.7	209.8 ± 17.1
89.7	90.5 ± 0.2	99.7 ± 1.8	107.7 ± 5.3	245.8 ± 19.8
101.4	102.2 ± 0.2	113. 0 ± 2.1	121.4 ± 6.0	287.4 ± 22.9
114.7	115.5 ± 0.2	127.9 ± 2.4	136.3 ± 6.8	335.5 ± 26.7
129.7	130.4 ± 0.3	144.9 ± 2.8	152.6 ± 8.0	390.8 ± 31.5
146.7	147.4 ± 0.3	164.2 ± 3.3	170.8 ± 9.6	454.6 ± 37.5
165.8	166.5 ± 0.3	186.0 ± 4.0	191.1 ± 11.7	527.1 ± 44.8
187.5	188.2 ± 0.4	210.6 ± 4.8	214.1 ± 14.3	610.2 ± 53.9
212.0	212.6 ± 0.4	238.6 ± 5.8	240.4 ± 17.4	704.6 ± 64.9
239.8	240.4 ± 0.5	270.3 ± 6.9	270.6 ± 21.2	812.4 ± 77.7
271.2	271.8 ± 0.5	306.1 ± 8.3	305.0 ± 25.6	934.3 ± 92.3
306.6	307.2 ± 0.6	346.5 ± 9.7	344.3 ± 30.8	1072.0 ± 108.9
346.7	347.5 ± 0.7	392.3 ± 11.4	389.3 ± 37.0	1228.6 ± 127.5
392.0	392.8 ± 0.8	443.9 ± 13.3	440.6 ± 44.1	1405.2 ± 148.3
443.2	444.1 ± 0.9	502.2 ± 15.4	499.0 ± 52.4	1604.7 ± 171.4
501.3	502.2 ± 1.1	568.3 ± 17.7	565.9 ± 61.9	1830.9 ± 197.0
566.8	567.9 ± 1.2	642.8 ± 20.2	642.0 ± 73.0	2086.0 ± 225.3
640.9	642.1 ± 1.4	727.1 ± 23.1	728.9 ± 85.8	2374.4 ± 256.9
724.7	726.0 ± 1.6	822.2 ± 26.3	828.1 ± 100.7	2699.7 ± 292.1
819.5	821.0 ± 1.8	929.8 ± 29.9	941.4 ± 118.0	3067.6 ± 331.2
926.6	928.4 ± 2.0	1051.3 ± 33.8	1070.9 ± 138.5	3481.9 ± 374.7

Table S 3. Regional and total deposition doses for children.

Child	Dose without hygroscopicity (10^8 particles d^{-1})			Dose considering hygroscopicity (10^8 particles d^{-1})			Impact of hygroscopicity on dose		
	hydrophobic	hygroscopic	sum	hydrophobic	hygroscopic	sum	hydrophobic	hygroscopic	sum
Head	0.54	5.39	5.95	0.54	5.46	6.01	0.34%	−1.29%	−0.94%
TB	3.22	28.99	32.26	3.05	21.41	24.46	5.18%	26.16%	24.16%
P	6.97	63.02	70.07	6.63	45.03	51.66	4.89%	28.54%	26.27%
Total	10.73	97.40	108.28	10.22	71.90	82.13	4.75%	26.18%	24.14%

Table S 4. Regional and total deposition doses for adults.

Adult	Dose without hygroscopicity (10^8 particles d^{-1})			Dose considering hygroscopicity (10^8 particles d^{-1})			Impact of hygroscopicity on dose		
	hydrophobic	hygroscopic	sum	hydrophobic	hygroscopic	sum	hydrophobic	hygroscopic	sum
Head	1.66	15.92	17.61	1.66	15.87	17.53	0.10%	0.33%	0.48%
TB	8.35	74.28	82.73	7.88	53.24	61.13	5.57%	28.32%	26.11%
P	12.81	114.90	127.84	12.16	82.57	94.72	5.09%	28.14%	25.90%
Total	22.82	205.10	228.18	21.70	151.68	173.38	4.90%	26.05%	24.02%

Table S 5. Regional and total deposition doses for the elderly group.

Elderly	Dose without hygroscopicity (10^8 particles d^{-1})			Dose considering hygroscopicity (10^8 particles d^{-1})			Impact of hygroscopicity on dose		
	hydrophobic	hygroscopic	sum	hydrophobic	hygroscopic	sum	hydrophobic	hygroscopic	sum
Head	1.61	15.49	17.13	1.60	15.52	17.12	0.31%	−0.15%	0.07%
TB	8.26	73.58	81.94	7.79	52.89	60.68	5.59%	28.12%	25.94%
P	13.24	118.79	132.16	12.55	85.28	97.83	5.18%	28.21%	25.97%
Total	23.11	207.86	231.24	21.94	153.69	175.63	4.99%	26.06%	24.04%

The particle number size distributions (PNSDs) of ambient aerosols during the daytime and nighttime are shown in Fig. S1. The particle number concentrations (PNCs) were $(1.99 \pm 1.28) \times 10^4$ and $(1.71 \pm 0.71) \times 10^4$ cm^{-3} in the day and at night, respectively.

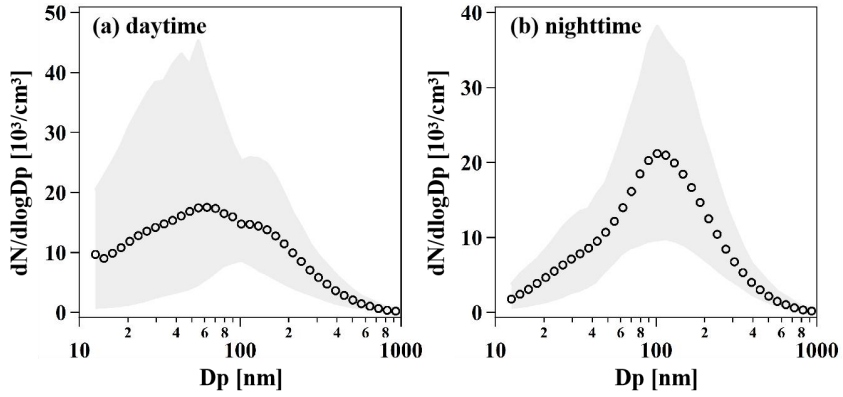

Figure S 1. The average particle number size distributions (PNSDs) measured by TDMPS (the black markers) during the (a) daytime (05:00–19:00 local time (LT; UTC+8)) and (b) nighttime (20:00–04:00LT on the next day). The upper and lower edges of the gray area represent the 90th and 10th quantiles of the PNSDs, respectively.

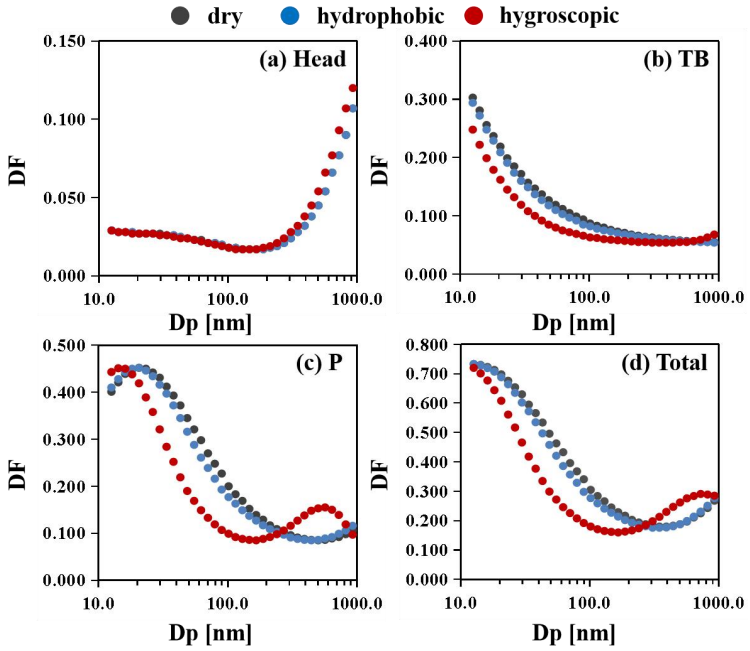

Figure S 2. Size-resolved (a) head, (b) TB, (c) P, and (d) total deposition fractions (DFs) of particles under dry conditions (i.e., without considering hygroscopicity), and hydrophobic and hygroscopic particles in humid environments (i.e., considering hygroscopicity) for children. The black, blue, and red dots represent dry, hydrophobic, and hygroscopic particles, respectively. In Fig. S2a, the black dots representing DFs under dry conditions is hidden behind the blue dots representing DFs of hydrophobic particles, because these two sets of DFs are close to each other.

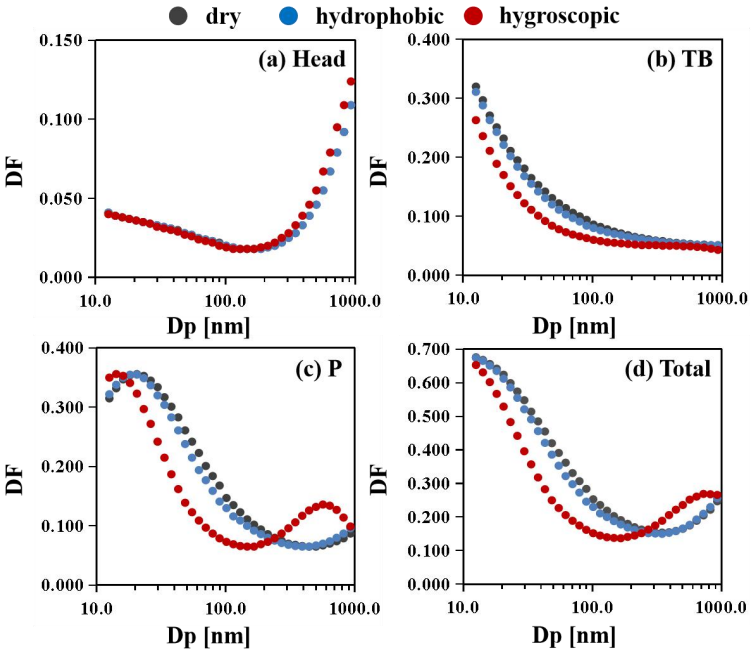

Figure S 3. Size-resolved (a) head, (b) TB, (c) P, and (d) total deposition fractions (DFs) of particles under dry conditions (i.e., without considering hygroscopicity), and hydrophobic and hygroscopic particles in humid environments (i.e., considering hygroscopicity) for the elderly group. The black, blue, and red dots represent dry, hydrophobic, and hygroscopic particles, respectively. In Fig. S3a, the black dots representing DFs under dry conditions is hidden behind the blue dots representing DFs of hydrophobic particles, because these two sets of DFs are close to each other.

The particle density mainly affects the probability of inertial impaction during the particle deposition process, which can be evaluated by using the dimensionless Stokes number (Stk), defined as Eq. (S1), as follows (Pramod et al., 2011):

$$\mathrm{Stk} = \frac{\rho_p d_p{}^2 C_c U}{18 \eta d_f} \quad \text{(S1)}$$

where ρ_p is the density of the particle. The Stokes number is the basic parameter describing the inertial impaction mechanism. A larger Stokes number implies a higher probability of deposition by impaction (Pramod et al., 2011).

Due to the lack of the density measurement of particles during the sampling period, the differences between the size-resolved DFs of particles with ρ_p = 1.0 g cm^{-3} vs. ρ_p = 1.5 g cm^{-3} for adults were compared. As displayed in Fig. S4, the particle density has great influence on the particle deposition in the head and P regions for larger submicron particles. The average DF differences in the head, TB, P, and the whole HRT were (11.1 ± 13.9)%, (0.5 ± 0.8)%, (3.8 ± 6.4)%, and (4.2 ± 6.5)%, respectively. Therefore, the measurement or estimation of the particle density during the particle hygroscopic growth is of great importance in calculating the particle deposition in human bodies.

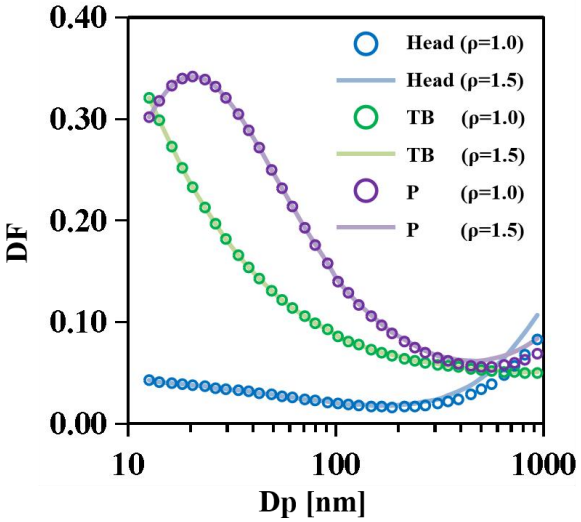

Figure S 4. Size-resolved regional deposition fractions (DFs) of particles with density (ρ) = 1.0 vs. 1.5 g cm^{-3} for adults. The blue, green, and purple markers represent the DFs of particles with ρ = 1.0 g cm^{-3} in the head, TB, and P, respectively. The blue, green, and purple lines represent the DFs of particles with ρ = 1.5 g cm^{-3} in the head, TB, and P, respectively.

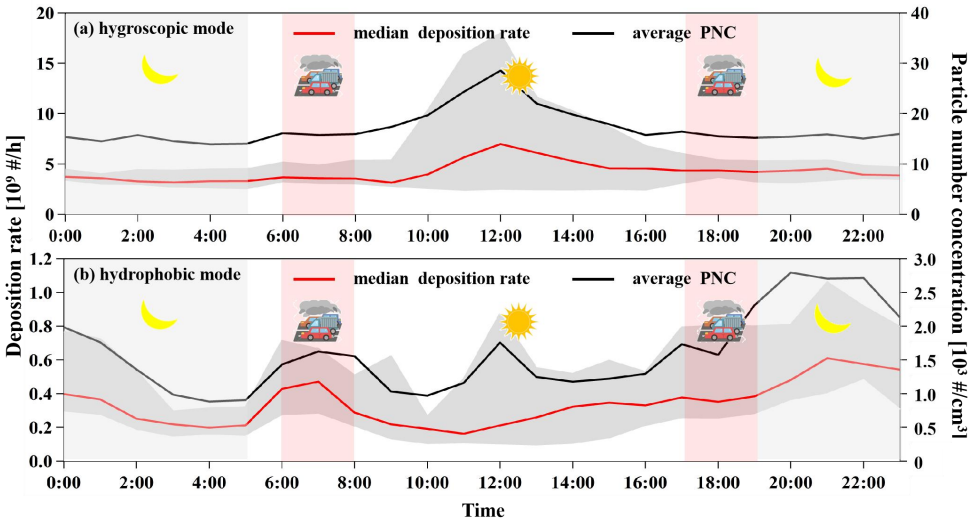

Figure S 5. The diurnal variations of deposition rates without considering hygroscopicity and the particle number concentrations (PNCs) of (a) hygroscopic and (b) hydrophobic particles for adults. The red lines represent the median deposition rate. The upper and lower edges of the gray area represent the 75th and 25th quantiles of deposition rates, respectively. The black lines represent the average PNC.

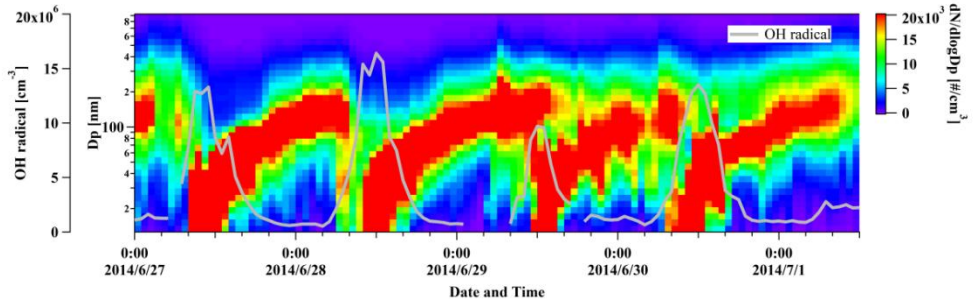

Figure S 6. The particle number size distribution of typical new particle formation events from June 27 to July 2, 2014. The gray line represents the concentrations of OH radical.

As shown in Fig. S7, a peak appeared at D_p = 2−3 μm in the DF curves of the head and P regions, which resulted in a peak in the total DF curve. It implied that particles with larger diameters may also have a significant contribution to the particle deposition in the human respiratory tract.

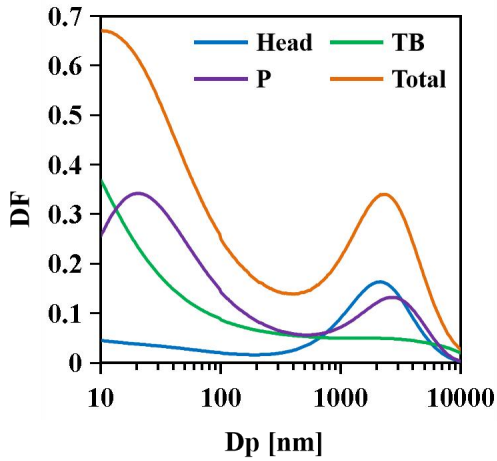

Figure S 7. The size-resolved regional and total DFs for adults. The particle density was set as 1.0 g cm^{-3}.

Reference

Liu, P. F., Zhao, C. S., Göbel, T., Hallbauer, E., Nowak, A., Ran, L., Xu, W. Y., Deng, Z. Z., Ma, N., Mildenberger, K., Henning, S., Stratmann, F., and Wiedensohler, A.: Hygroscopic properties of aerosol particles at high relative humidity and their diurnal variations in the North China Plain, Atmospheric Chemistry and Physics, 11, 3479-3494, 10.5194/acp-11-3479-2011, 2011.

Pramod, K., Paul B., and Klaus W.: Aerosol measurement: principles, techniques, and applications (Third Edition), John Wiley & Sons, Inc, Hoboken, the United States, 2011.

Shi, J., Hong, J., Ma, N., Luo, Q., He, Y., Xu, H., Tan, H., Wang, Q., Tao, J., Zhou, Y., Han, S., Peng, L., Xie, L., Zhou, G., Xu, W., Sun, Y., Cheng, Y., and Su, H.: Measurement report: On the difference in aerosol hygroscopicity between high and low relative humidity conditions in the North China Plain, Atmospheric Chemistry and Physics, 22, 4599-4613, 10.5194/acp-22-4599-2022, 2022.

Sun, Y. L., Wang, Z. F., Du, W., Zhang, Q., Wang, Q. Q., Fu, P. Q., Pan, X. L., Li, J., Jayne, J., and Worsnop, D. R.: Long-term real-time measurements of aerosol particle composition in Beijing, China: seasonal variations, meteorological effects, and source analysis, Atmospheric Chemistry and Physics, 15, 10149-10165, 10.5194/acp-15-10149-2015, 2015.

Swietlicki, E., Hansson, H. C., Hameri, K., Svenningsson, B., Massling, A., McFiggans, G., McMurry, P. H., Petaja, T., Tunved, P., Gysel, M., Topping, D., Weingartner, E., Baltensperger, U., Rissler, J., Wiedensohler, A., and Kulmala, M.: Hygroscopic properties of submicrometer atmospheric aerosol particles measured with H-TDMA instruments in various environments - a review, Tellus Series B-Chemical and Physical Meteorology, 60, 432-469, 10.1111/j.1600-0889.2008.00350.x, 2008.

Zhang, S. L., Ma, N., Kecorius, S., Wang, P. C., Hu, M., Wang, Z. B., Größ, J., Wu, Z. J., and Wiedensohler, A.: Mixing state of atmospheric particles over the North China Plain, Atmospheric Environment, 125, 152-164, 10.1016/j.atmosenv.2015.10.053, 2016.